DRAFT VERSION MARCH 25, 2013
Preprint typeset using LaTeX style emulateapj v. 2/16/10

arXiv:1303.5443v1 [astro-ph.CO] 21 Mar 2013

TOWARD A COMPREHENSIVE MODEL FOR FEEDBACK BY ACTIVE GALACTIC NUCLEI: NEW INSIGHTS FROM M87 OBSERVATIONS BY LOFAR, *Fermi* AND H.E.S.S.

CHRISTOPH PFROMMER
Heidelberg Institute for Theoretical Studies, Schloss-Wolfsbrunnenweg 35, D-69118 Heidelberg, Germany

Draft version March 25, 2013

ABSTRACT

Feedback by active galactic nuclei (AGN) appears to be critical in balancing radiative cooling of the low-entropy gas at the centers of galaxy clusters and in mitigating the star formation of elliptical galaxies. New observations of M87 enable us to put forward a comprehensive model for the physical heating mechanism. Low-frequency radio observations by LOFAR revealed the absence of *fossil* cosmic ray (CR) electrons in the radio halo surrounding M87. This puzzle can be resolved by accounting for the CR release from the radio cocoons and the subsequent mixing of CRs with the dense ambient intracluster gas, which thermalizes the electrons on a timescale similar to the radio halo age of 40 Myrs. Hadronic interactions of similarly injected CR protons with the ambient gas should produce an observable gamma-ray signal in accordance with the steady emission of the low state of M87 detected by *Fermi* and H.E.S.S. Hence, we normalize the CR population to the gamma-ray emission, which shows the same spectral slope as the CR injection spectrum probed by LOFAR, thereby supporting a common origin. We show that CRs, which stream at the Alfvén velocity with respect to the plasma rest frame, heat the surrounding thermal plasma at a rate that balances that of radiative cooling *on average* at each radius—thereby setting the thermal pressure profile equal to that of the streaming CRs. However, the resulting global thermal equilibrium is locally unstable and allows for the formation of the observed cooling multi-phase medium through thermal instability. Provided CR heating balances cooling during the emerging "cooling flow", the collapse of the majority of the gas is halted at 1 keV, which is in accordance with x-ray data. We show that both the existence of a temperature floor and the similar radial scaling of the heating and cooling rates are generic predictions of the CR heating model.

Subject headings: cosmic rays — galaxies: active — galaxies: clusters: intracluster medium — galaxies: individual (M87) — gamma rays: galaxies: clusters — radio continuum: galaxies

1. INTRODUCTION

The central cooling time of the x-ray emitting gas in galaxy clusters and groups is bimodally distributed; approximately half of all systems have radiative cooling times of less than 1 Gyr and establish a population of cool core (CC) clusters (Cavagnolo et al. 2009). In the absence of any heating process, these hot gaseous atmospheres are expected to cool and to form stars at rates up to several hundred $\mathrm{M}_\odot\ \mathrm{yr}^{-1}$ (see Peterson & Fabian 2006, for a review). Instead, the observed gas cooling and star formation rates are reduced to levels substantially below those expected from unimpeded cooling flows. High-resolution *Chandra* and *XMM-Newton* observations show that while the gas temperature is smoothly declining toward the center, there is a lack of emission lines from gas at a temperature below about one third of the ambient cluster temperature (Peterson et al. 2003; Peterson & Fabian 2006). Apparently, radiative cooling is offset by a yet to be identified heating process that is associated with the AGN jet-inflated radio cocoons that are co-localized with the cavities seen in the x-ray maps. The interplay of cooling gas, subsequent star formation and nuclear activity appears to be tightly coupled to a self-regulated feedback loop (for reviews, see McNamara & Nulsen 2007, 2012). Feedback is considered to be a crucial if not unavoidable process of the evolution of galaxies and supermassive black holes (Croton et al. 2006; Puchwein & Springel 2013). While the energetics of AGN feedback is sufficient to balance radiative cooling, it is unable to transform CC into non-CC clusters on the buoyancy timescale due to the weak coupling between the mechanical energy to the cluster gas (Pfrommer et al. 2012). Matching this observational fact has proven to be difficult in cosmological simulations of AGN feedback that include realistic metal-line cooling (Dubois et al. 2011).

Several physical processes have been proposed to be responsible for the heating, including an inward transport of heat from the hot outer cluster regions (Narayan & Medvedev 2001), turbulent mixing (Kim & Narayan 2003), redistribution of heat by buoyancy-induced turbulent convection (Chandran & Rasera 2007; Sharma et al. 2009), and dissipation of mechanical heating by outflows, cocoons, or sound waves from the central AGN (e.g., Churazov et al. 2001; Brüggen & Kaiser 2002; Ruszkowski & Begelman 2002; Ruszkowski et al. 2004). The total energy required to inflate a cavity of volume V in an atmosphere of thermal pressure P_{th} is equal to its enthalpy $E_{\mathrm{cav}} = \gamma/(\gamma-1)\,P_{\mathrm{th}}V = 4\,P_{\mathrm{th}}V$, assuming a relativistic equation of state with $\gamma = 4/3$ within the cocoons. Hence, the dissipation of mechanical energy resulting from the volume work done on the surroundings only makes use of one quarter of the total available enthalpy. Only a fraction thereof is dissipated in the central regions, which have the smallest cooling time (since most of the temperature increase caused by weak shocks is provided adiabatically).

It would be more economic to additionally use the remaining part that is stored in the internal energy of the (presumably) relativistic particle population. *If* those CRs were mixed into the ambient gas, there would be a promising process to transfer CR into thermal energy. Fast streaming CRs along the magnetic field excite Alfvén waves through the "streaming instability" (Kulsrud & Pearce 1969). Scattering off this wave field effectively limits the bulk speed of CRs. Damping of these waves transfers CR energy and momentum to the thermal gas at a rate that scales with the CR pressure gradient. Hence, this could provide an efficient means of suppressing the cooling catastrophe of CCs (Guo & Oh 2008; Enßlin et al. 2011; Fujita & Ohira 2012; Wiener et al. 2013), but only *if* the CR pressure gradient is sufficiently large.

This work studies the consequences of this CR-heating model with the aim of putting forward an observationally well-founded and comprehensive model. In particular, we intend to eliminate two of the most uncertain assumptions of this process, the mixing of CRs with the ambient plasma and the CR abundance in the central cluster regions. Moreover, we tackle the question about thermal balance in the core region of a CC cluster, but constrained to this model in which CR Alfvén wave heating competes with radiative cooling. To this end, we focus on the closest active galaxy that is interacting with the cooling cluster gas that provides us with the most detailed view on AGN feedback possible. This selects M87, the cD galaxy of the Virgo cluster at a distance of 16.7 ± 0.2 Mpc (Mei et al. 2007), where $1'$ corresponds to 4.85 kpc. It is well-studied not only at x-rays (e.g., Million et al. 2010) but also and especially at non-thermal wave lengths, i.e., in the radio (Owen et al. 2000; de Gasperin et al. 2012) and γ-ray regime (Rieger & Aharonian 2012).

In Section 2 we show how new observations of M87 by LOFAR, *Fermi*, and H.E.S.S. can shed light on the injection and mixing of CRs into the ambient plasma and estimate the CR pressure contribution in the central regions. Section 3 discusses the balance of CR heating with radiative cooling. Particular attention is paid to local thermal stability of the global thermal equilibrium that we find. In Section 4 we present predictions of our model that include gamma-ray, radio, and Sunyaev-Zel'dovich observations and discuss how those can be used to quantify open aspects of the presented heating mechanism. Finally, we compare our model with other solutions to the "cooling flow problem" and conclude in Section 5. In Appendix A, we derive a thermal instability criterion for a fluid that is cooling by thermal bremsstrahlung and line emission and is heated by a generic mechanism while allowing for thermal and CR pressure support.

2. A NON-THERMAL MULTI-MESSENGER APPROACH

2.1. *Cosmic-Ray Injection: Insights by LOFAR*

The characteristic frequency ν_s at which a CR electron (CRe) emits synchrotron radiation scales with the magnetic field strength B and the CRe's cooling time τ as $\nu_s \propto B^{-3}\tau^{-2}$ (assuming the strong-field limit for which inverse Compton cooling is negligible). Hence, observations at lower radio frequencies should enable to probe older fossil CRe populations. Those are expected to accumulate at lower energies, which would imply a low-frequency spectral steepening. Equivalently, such observations should unveil the time-integrated non-thermal action of AGN feedback that is expected to be spread out over larger spatial scales. However, recent LOFAR observations of Virgo A, the radio source of M87, provided two unexpected findings. (1) The observations do not reveal a previously hidden spectral steepening toward low frequencies and show the extended radio halo to be well confined within boundaries that are identical at all frequencies (de Gasperin et al. 2012). The possibility that this may point to a special time, which is characterized by a recent AGN outburst after long silence, is unlikely because statistical studies of the radio-mode feedback in complete samples of clusters imply that the duty cycle of AGN outbursts with the potential to heat the gas significantly in CC clusters is $\geq 60\%$ and could approach unity after accounting for selection effects (Bîrzan et al. 2012). (2) While the core region displays a radio spectral index[1] of $\alpha_\nu = 0.6 \pm 0.02$ (consistent with an injection CR spectral index of $\alpha = 2\alpha_\nu + 1 = 2.2 \pm 0.04$), the low-frequency halo spectrum outside the central cocoon is considerably steeper with $\alpha_\nu = 0.85$. As suggested by de Gasperin et al. (2012), the most probable explanation of this steepening at low frequencies is strong adiabatic expansion in combination with a superposition of differently synchrotron-aged CRe populations. Adiabatic expansion across a density expansion factor $f = \rho_2/\rho_1$ from the compact source to the more dilute halo regions shifts all CR momenta by the factor $p_2 = f^{1/3} p_1$. CRes that are leaving the cocoon regions have spent different time intervals in regions of strong magnetic fields, which leads to a distribution of spectra with different break momenta. Superposition of those spectra steepens the spectrum down to low frequencies *if* the cooling time of the most strongly cooled CRes has been comparable to the transport time from the core to the current emitting region.

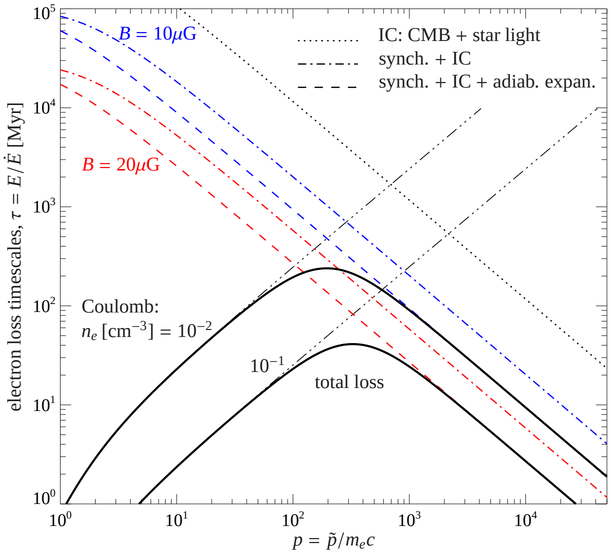

Figure 1. Cooling time of electrons for typical conditions in the central region of M87 as a function of normalized electron momentum, where $\tilde{p}$ is the physical momentum. During their advective transport in the radio cocoon, the (high-energy) electrons experience inverse Compton (IC), synchrotron, and adiabatic losses, for which we assume an expansion factor of $f = 10$. After the electrons mix with the ambient thermal plasma, Coulomb interactions can thermalize them. Electrons with kinetic energy $E \simeq p m_e c^2 \simeq 150$ MeV are the most long-lived, with a maximum cooling time of $\tau \simeq 40$ Myr that corresponds to the radio halo age.

In Fig. 1, we show the cooling time of CRes (see Pfrommer et al. 2008, for definitions). CRes of energy ~ 200 (400) MeV that are responsible for ~ 25 (100) MHz radio emission in a 20μG field have energy loss timescales of ~ 150 (75) Myr, which drops further by the factor $f^{1/3}$ after accounting for adiabatic expansion. CRes can cool through inverse Compton (IC) interactions with various seed photon fields, including the cosmic microwave background (CMB), star light, and dust-reprocessed infra-red emission. Within the central radio halo region ($r < 34$ kpc), the star formation-induced photon fields at least contribute as much as the CMB (Pinzke et al. 2011), which motivates our choice of a seed photon energy density that is twice that of the CMB. Synchrotron cooling in equipartition magnetic fields of $10-20\,\mu$G

---

[1] We define spectral indexes according to $F_\nu \propto \nu^{-\alpha_\nu}$.

(de Gasperin et al. 2012) and adiabatic expansion substantially decreases the cooling times further during the advective transport of CRes in the radio cocoons. Those rise in the cluster atmosphere (either buoyantly or driven by the jet) and uplift dense gas from the central regions (Werner et al. 2010). Those rising motions of light relativistic fluid cause strong downdrafts at the sides of the cocoons, which induce Rayleigh-Taylor and Kelvin-Helmholtz instabilities that shred the cocoons and excite turbulence, which mixes the CRes with the dense uplifted ambient plasma. This picture appears to be supported by radio maps of M87 (Owen et al. 2000; de Gasperin et al. 2012) that show a diffusely glowing radio halo surrounding the cocoons, which themselves show the characteristic mushroom shape of a Rayleigh-Taylor instability. Coulomb interactions of the released CRes with the dense ambient intracluster medium (ICM) cause them to be thermalized after a maximum cooling time of $\tau \simeq 40$ Myr, which corresponds to the radio halo age (see Fig. 1). Thus, this naturally explains the absence of a fossil CRe signature in the low-frequency radio spectra as well as the spatially similar morphology of Virgo A at all frequencies.

Diffusive shock acceleration operates identically on relativistic particles of the same rigidity ($R = \tilde{p}c/ze$, where $\tilde{p}$ is the physical momentum and z is the ion charge) and unlike electrons, protons do not suffer an injection problem into the acceleration process and have negligible radiative losses. Hence we expect CR protons (CRps) to dominate the pressure of the cocoons[2] and to exhibit a similar injection spectrum as the CRes in the central regions ($\alpha \approx 2.2$). Similarly to the CRes, CRps should also be released from the cocoons and mixed into the ambient ICM. Since adiabatic expansion leaves their spectral shape invariant and CRps have negligible radiative losses, we do not expect a spectral steepening of the CRp population in the halo. A necessary consequence of this picture are hadronic interactions of CRps with the ambient gas. This should produce a steady gamma-ray signal from M87 (Pfrommer & Enßlin 2003), with a spectral index above GeV energies of $\alpha_\gamma = \alpha \approx 2.2$.

2.2. *Cosmic-Ray Pressure Estimates from* Fermi *and H.E.S.S.*

To test this hypothesis, we turn to the gamma-ray regime. A joined unbinned likelihood fit with a power-law ($dN/dE \propto E^{-\alpha_\gamma}$) to the *Fermi* and H.E.S.S. data of M87's low state yields $F(>1\ \mathrm{GeV}) = 1.35(\pm 0.35)\times 10^{-9}$ photons cm^{-2} s^{-1} and $\alpha_\gamma = 2.26 \pm 0.13$ (Abdo et al. 2009), which is consistent with our expectation if the gamma-rays are produced in hadronic CRp-p interactions. Moreover, a comparison of the *Fermi* light curve for the last 14 months with the initial 10-months data revealed no evidence of variability in the flux above 100 MeV (Abramowski et al. 2012; Abdo et al. 2009).[3] Gamma-ray upper limits on M87 set by EGRET (Reimer et al. 2003) are consistent with the steady flux seen by *Fermi*. This demonstrates that the EGRET and *Fermi* observations of M87, which together span more than two decades, show no apparent increase in flux. Additionally, the *low flux state* at very high energies $E > 100$ GeV does not provide any hint of variability (Aharonian et al. 2006), although the low signal statistics renders such a test very difficult. Encouraged by the spectral similarity of radio and gamma-ray observations and the constant gamma-ray flux, we will now assume that the gamma rays are tracing hadronic CR interactions.

To estimate the CR pressure that is implied by the observed gamma-ray emission, we choose a constant CR-to-thermal pressure ratio, $X_{\mathrm{CR}} = P_{\mathrm{CR}}/P_{\mathrm{th}}$ (which we require for self-consistency as we will see in Section 3). We assume a CR power-law population,

$$\frac{d^4N}{dp\,d^3x} = Cp^{-\alpha}\theta(p-q), \tag{1}$$

where θ denotes the Heaviside step function and $\alpha = 0.226$. We decided in favor of the spectral index of the gamma-ray emission, which likely probes the prevailing CRp distribution in the radio halo region. In contrast, the radio emission of the central cocoon region may signal current acceleration conditions that, albeit generally very similar, may be slightly different from the ones that have accelerated the CRs in the past, which have now been released.

We use a fit to the spherically symmetric thermal pressure profile as inferred from x-ray observations (Matsushita et al. 2002; Böhringer et al. 1994). The thermal pressure is $P_{\mathrm{th}} = nkT = n_e kT/\mu_e$, where $\mu_e = n_e/n = \mu(X_{\mathrm{H}}+1)/2 \simeq 0.517$ for a fully ionized gas of primordial element composition with a hydrogen mass fraction $X_{\mathrm{H}} = 0.76$ and mean molecular weight $\mu = 0.588$. The electron density and temperature profiles[4] of the central region of the Virgo cluster ($r \lesssim 100$ kpc corresponding to $20'$) are given by fits to the x-ray profiles and have the form

$$n_e(r) = \left[\sum_{i=1}^{2} n_i^2 \left(1+\frac{r^2}{r_i^2}\right)^{-3\beta_i}\right]^{1/2}, \text{ and} \tag{2}$$

$$T_e(r) = T_0 + (T_1 - T_0)\left[1+\left(\frac{r}{r_t}\right)^{-1}\right]^{-1}, \tag{3}$$

where $(n_1, n_2) = (0.15, 0.013)$ cm^{-3}, $(r_1, r_2) = (1.6, 20)$ kpc, $(\beta_1, \beta_2) = (0.42, 0.47)$, $(kT_0, kT_1) = (1, 3)$ keV, and $r_t = 13.5$ kpc.

The sharp drop of radio morphology of Virgo A's halo suggests that the CRps are also confined to a central region of radius $r_{\max} = 34$ kpc. Hence we integrate the gamma-ray flux due to hadronic CRp-p interactions from within a spherical region bounded by $r_{\max}$. We use a semi-analytic formalism (Pfrommer & Enßlin 2004) that has been modified to constrain the CR-to-thermal *pressure* ratio (Pfrommer et al. 2008). We obtain $X_{\mathrm{CR}} = 0.38$ for a vanishing low-momentum cutoff, $q = 0$. Accounting for a non-zero low-momentum cutoff of the CRp distribution as a result of Coulomb cooling, we obtain $X_{\mathrm{CR}} = 0.31\ (0.34)$ for $q = 0.58\ (0.25)$ which corresponds to a Coulomb cooling time of CRps of $\tau = 40$ Myr, assuming an ambient electron density of $n_e = 10^{-1}\ \left(10^{-2}\right)$ cm^{-3}. Since there is considerable uncertainty about the shape of the low-momentum regime of the CR distribution function, we decided to adopt the most conservative value of $X_{\mathrm{CR}} = 0.31$ for the reminder of this work. We note that a fresh supply of CRps could lower q and therefore increase the CR pressure.

We checked that the radio emission from secondary CRes, which are inevitably injected by hadronic CRp-p reactions, has a subdominant contribution to the observed radio emission. While the total radio emission due to secondaries is well below the observed flux density of the radio halo of M87, future high-frequency observations at $\gtrsim 10$ GHz of the external halo parts may be able to probe the hadronically-induced radio emission (see Section 4.2 for more details). At these frequencies, the hadronically-induced emission component cannot any more be neglected and complicates inferences on the CRe pitch angle distribution in different spectral ageing models of radio-emitting CRes.

---

[2] In fact, α-particles carry a significant fraction of the total CR energy, which we absorb into the proton spectrum with the following line of reasoning. A GeV energy α-particle can be approximated as an ensemble of four individual nucleons travelling together due to the relatively weak MeV nuclear binding energies in comparison to the kinetic energy of relativistic protons. See Enßlin et al. (2007) for an extended discussion.

[3] A light curve analysis of 4 years of *Fermi* data does not show any sign of variability either (F. Rieger, priv. comm.).

[4] In Virgo, the gas is observed to have a maximum temperature $T \simeq 3\times 10^7$ K at a cluster-centric radius of ~ 200 kpc (corresponding to $40'$, Böhringer et al. 1994).

In general, cluster merger and accretion shocks are also expected to accelerate CRs, which add to the CR population injected by the central AGN. Non-observations of gamma-ray emission at GeV and TeV energies limits their contribution to $X_{\rm CR} < 0.017$ in the Coma and Perseus clusters (Arlen et al. 2012; Aleksić et al. 2012) and typically to less than a few per cent for the next to best targets (Ackermann et al. 2010; Pinzke et al. 2011). We hence neglect their contribution in the center, where the AGN-injected population apparently dominates.

These findings for $X_{\rm CR}$ are in agreement with constraints on the non-thermal pressure contribution in M87 that have been derived by comparing the gravitational potentials inferred from stellar and globular cluster kinematics and from assuming hydrostatic equilibrium of the x-ray emitting gas (Churazov et al. 2010). Depending on the adopted estimator of the optical velocity dispersion, they find a non-thermal pressure bias of $X_{\rm nt} = P_{\rm nt}/P_{\rm th} \approx 0.21-0.29$ (which is even higher in M87 for more sophisticated estimates that are less sensitive to the unknown orbit anisotropy). There are several effects that could (moderately) increase $X_{\rm nt}$. (1) A more extended distribution of $P_{\rm nt}$ in comparison to $P_{\rm th}$ could hide a larger non-thermal pressure contribution (since only the pressure gradient enters into the equation for hydrostatic equilibrium), (2) the presence of an x-ray "invisible" cool gas phase that is coupled to the hot phase could bias $X_{\rm nt}$ low (Churazov et al. 2008), and (3) the tension in the orbit anisotropy estimates of the stars and globular clusters may call for triaxial potential models (Romanowsky & Kochanek 2001).

2.3. *Pressure Content of Radio Cocoons*

So far, we implicitly assumed that the pressure of radio cocoons is provided by a relativistic component. While it is unknown what physical component provides the dominant energetic contribution to radio cocoons, here we will review the reasons for our assumption. Equipartition arguments for the radio emitting cocoons show that the sum of CRes and magnetic fields can only account for a pressure fraction of $\simeq 10\%$ in comparison to the external pressure, with which the cocoons are apparently in approximate hydrostatic equilibrium (Blanton et al. 2003; de Gasperin et al. 2012). However, these estimates rely on power-law extrapolations from the high-energy part of the CRe distribution (with Lorentz factor $\gamma \gtrsim 10^3$, which was visible so far at radio frequencies $\nu \gtrsim 300$ MHz) to lower energies which dominate the CRe energy budget, leaving the possibility of an aged fossil CRe population that would dominate the pressure. LOFAR observations have now unambiguously demonstrated the absence of such a hypothetical fossil CRe population in M87 (de Gasperin et al. 2012). Since CRps should be accelerated at least as efficiently as the visible CRes and since CRps have negligible radiative cooling rates (in comparison to CRes), we make the very plausible assumption in this work that CRps provide the dominating pressure component of cocoons (and work out a few smoking-gun tests for this scenario in Section 4). The alternative scenario of a hot, but subrelativistic (Maxwellian) proton population is unlikely because of three reasons. (1) CRp Coulomb cooling time scales are too short (see, e.g., Enßlin et al. 2007), implying a burst-like heating once the content has been set free as a result of shredding the radio cocoons by the action of Kelvin-Helmholtz and Rayleigh-Taylor instabilities. However, there is no signature in the x-ray observations of such a localized heating around the shredded cocoons (Million et al. 2010). (2) Moreover, LOFAR observations show no sign of such a ~ 100 MeV electron distribution, requiring a helicity fine-tuning for the acceleration process. (3) Adiabatic expansion of a composite of relativistic and non-relativistic (thermal) populations favors the CR over the non-relativistic population since $P_{\rm CR}/P_{\rm th} \propto f^{-1/3}$, due to the softer equation of state of CRs. Here we assumed an ultra-relativistic CR population with an adiabatic exponent of $\gamma = 4/3$ and $f = \rho_2/\rho_1$ is the density expansion factor starting from the densities at which the two populations got energized.

3. COSMIC-RAY HEATING VERSUS RADIATIVE COOLING

The previous arguments provide strong evidence that CRs are released from the radio cocoons of M87 and mixed into the ICM on a time scale of $\tau \simeq 40$ Myr. Interpreting the observed gamma-ray emission as a signature of hadronic CRp-p interactions enabled us to estimate the CR pressure contribution. We now turn to the question whether the resulting CR Alfvén wave heating is powerful enough to balance radiative cooling and what this may imply for thermal stability of the gas in M87 and CCs in general.

3.1. *Cosmic-Ray Heating*

Advection of CRs by the turbulent gas motions produces centrally enhanced profiles. In contrast, CR streaming along magnetic field lines implies a net outward flux of CRs that causes the profiles to flatten (Enßlin et al. 2011). A necessary requirement for CR streaming to work is a centrally peaked profile of the CR number density. Do we have any evidence for this in M87? Radio maps of Virgo A (Owen et al. 2000; de Gasperin et al. 2012) suggest that turbulent advection, driven by the rising cocoons, is strong enough to maintain a sufficiently strong inward transport of CRs. Alternatively, the smoothly glowing radio halo that fills the central region for $r < r_{\rm max}$ may be caused by escaping CRs from the cocoons already at the early stages of their rise. Following observational and theoretical arguments, the current distribution of the CR pressure appears to follow a centrally peaked profile.

The CR Alfvén wave heating term is given by (Wentzel 1971; Guo & Oh 2008)

$$\mathcal{H}_{\rm CR} = -\upsilon_A \nabla P_{\rm CR} = -\upsilon_A \left(\nabla_r \langle P_{\rm CR} \rangle_\Omega + \frac{\delta P_{\rm CR}}{\delta l} \right), \qquad (4)$$

where $\upsilon_A = B/\sqrt{4\pi\rho}$ is the Alfvén velocity, ρ is the gas mass density, and we decompose the local CR pressure gradient into the radial gradient of the azimuthally averaged CR pressure profile, $\langle P_{\rm CR} \rangle_\Omega$, and a fluctuating term, $\delta P_{\rm CR}/\delta l \equiv \nabla P_{\rm CR} - \nabla_r \langle P_{\rm CR} \rangle_\Omega$, which in general also points in non-radial direction. In steady state, CR streaming transfers an amount of energy to the gas per unit volume of

$$\Delta\varepsilon_{\rm th} = -\tau_A \upsilon_A \nabla P_{\rm CR} \approx P_{\rm CR} = X_{\rm CR} P_{\rm th}, \qquad (5)$$

where we used the Alfvén crossing time $\tau_A = \delta l/\upsilon_A$ over the CR pressure gradient length, δl. Comparing the first and last term of this equation suggests that a constant CR-to-thermal pressure ratio is a necessary condition if CR streaming is the dominant heating process, i.e., the thermal pressure profile adjusts to that of the streaming CRs in equilibrium so that we will take the radial profile of $P_{\rm th}$ as a proxy for $P_{\rm CR}$.

The observed radial profile of $P_{\rm th}$ averages over the local pressure inhomogeneities within a given radial shell, especially toward the center where the azimuthally averaged radial profile plateaus out. However, such a constant $P_{\rm th}$ at the center is in strong disagreement with the fluctuating thermal pressure maps (see Fig. 7 of Million et al. 2010). Those pressure fluctuations could have their origin in shocks, turbulence, perturbations of the gravitational potential, or entropy variations of advected gas that has not had time to come into pressure equilibrium with the surroundings. To illustrate one of these possibilities, we consider pressure fluctuations due to weak shocks and expand the Rankine-Hugoniot jump conditions in the limit of small Mach number, $\mathcal{M}_1 - 1 = \varepsilon \ll 1$:

$$\frac{P_2}{P_1} = \frac{2\gamma\mathcal{M}_1^2 - (\gamma - 1)}{\gamma + 1} \approx 1 + \frac{4\gamma}{\gamma + 1}\,\varepsilon = 1 + \frac{5}{2}\,\varepsilon, \tag{6}$$

where subscripts 1 and 2 denote upstream and downstream quantities in the shock rest frame and we assume $\gamma = 5/3$ in the third step. Adopting a constant CR-to-thermal pressure ratio, we obtain an estimate for the CR heating due to pressure fluctuations as a result of a sequence of weak shocks, i.e., the second term on the right-hand side of Equation (4)

$$\frac{\delta P_{\rm CR}}{\delta l} \approx -\frac{5}{2}\,\frac{\varepsilon X_{\rm CR} P_{\rm th}}{r}. \tag{7}$$

Here we assume that the characteristic size scale of the pressure fluctuations is of order the cluster-centric radius, which can be realized, e.g., for spherically symmetric shocks whose curvature radius increases as r. We note, that some of the other mechanisms that may be responsible for the observed pressure fluctuations can in principle have a different scaling with radius and hence, have a modified radial dependence of the fluctuating term in $\mathcal{H}_{\rm CR}$, in particular at the center. It will be subject to future work to quantify the contribution of those processes to the CR heating rate.

We choose conservative values for the magnetic field strengths that are about half as much as the minimum energy estimates presented in de Gasperin et al. (2012). We adopt $B = 20\,\mu{\rm G}\,\sqrt{n_e/0.1{\rm cm}^{-3}}$, which yields $B = 24$ (5) μG for the central value (at the halo boundary, $r_{\rm max} = 34$ kpc). The density scaling yields a constant Alfvén velocity $\upsilon_A \approx 130$ km s^{-1}. The plasma beta factor $\beta = P_{\rm th}/P_B$ increases from 11 (at the center) to 28 (at $r_{\rm max}$), which corresponds to a magnetic pressure contribution of $X_B = 0.08$ (center) and 0.035 ($r_{\rm max}$).

3.2. *Global Thermal Equilibrium*

Radiative cooling of cluster gas is dominated by thermal bremsstrahlung and collisional excitation of heavy ions to metastable states and the subsequent line emission following de-excitation (the latter of which dominates for particle energies $\lesssim 3$ keV). These processes are characterized by the cooling rate

$$\mathcal{C}_{\rm rad} = n_e n_t \Lambda_{\rm cool}(T, Z), \tag{8}$$

where the target density n_t is the sum of ion densities and we defined the cooling function $\Lambda_{\rm cool}(T, Z)$ that depends on temperature T and metal abundance Z. The cooling function is fairly flat between the range of temperatures of $kT_0 = (1-2)$ keV, we encounter in the central regions, bounded by the radio halo. The X-ray inferred metallicity map shows substantial spatial variations on small scales ranging in between $Z_0 = (0.7-1.3)\,Z_\odot$, which are of similar amplitude as the overall radial trend in Z (Million et al. 2010). Hence, we decided to bracket the cooling function for these ranges of temperature and metallicity, which yields $\Lambda_{\rm cool}(T_0, Z_0) \approx (1.8-2.8) \times 10^{-23}$ erg cm^3 s^{-1} while assuming collisional ionization equilibrium (see Fig. 8 of Sutherland & Dopita 1993).

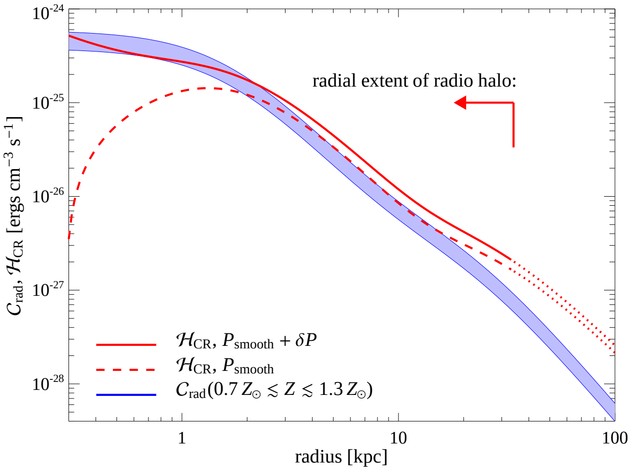

Figure 2. CR heating versus radiative cooling rates. The cooling rates (blue) account for a fluctuating metal distribution in the range $(0.7-1.3)\,Z_\odot$ and are globally balanced at each radius by CR Alfvén wave heating. We show the CR heating rate $\mathcal{H}_{\rm CR}$ due to the azimuthally averaged pressure profile that "smoothes" out the CR pressure gradient (dashed red) and the $\mathcal{H}_{\rm CR}$ profile, where we additionally account for pressure fluctuations due to weak shocks of typical Mach number $\mathcal{M} = 1.1$ (solid red). The CR heating rates become very uncertain outside the boundary of the radio halo of Virgo A (indicated with a dotted red).

Figure 2 shows the radial profile of the radiative cooling rate $\mathcal{C}_{\rm rad}$ and that of the CR heating rate $\mathcal{H}_{\rm CR}$. For radii $r \gtrsim 2$ kpc, CR heating balances cooling already for the "smoothed" gradient pressure term $(\nabla_r \langle P_{\rm CR} \rangle_\Omega)$. The central pressure plateau causes the CR pressure gradient and hence, the CR heating to drop. To model the large visible fluctuations in $P_{\rm th}$ (and hence in $P_{\rm CR}$ according to Equation 5), we assume that they are caused by weak shocks of typical Mach number $\mathcal{M} = 1.1$ with a size scale that is of order the radius (i.e., we adopt $\varepsilon = 0.1$ in Equation 6). This fluctuating pressure term appears to be critical in balancing the cooling rate with CR heating in the central region for $r < 2$ kpc. We conclude that CR Alfvén wave heating can globally balance cooling, hence justifying our assumption of a constant CR-to-thermal pressure. Particularly notable is the non-trivial result that the radial shapes of $\mathcal{C}_{\rm rad} \propto n^2$ and $\mathcal{H}_{\rm CR} \propto \nabla_r P_{\rm th}$ closely track each other. In fact, if CR heating dominates, $P_{\rm th}$ should be determined by the pressure profile of the streaming CRs and hence this resemblance of the radial heating and cooling rate profiles is an important signature of self-consistency. The sharp boundaries of the radio halo of Virgo A may suggest that CRs are confined to within its boundaries, perhaps as a result of azimuthally wrapped magnetic fields. Hence the CR heating rates become very uncertain outside the maximum halo radius.

We will argue that this similarity of the CR heating and radiative cooling profiles is not a coincidence in M87, but rather generically expected in models of CR Alfvén wave heating.

For simplicity, we use a constant gas-to-dark matter ratio inside the dark-matter scale radius, i.e., $n \propto r^{-1}$, which is characteristic for the central density profile in CCs. Outside the temperature floor, we adopt a temperature profile with a small positive slope, $T \propto r^{\alpha_t}$ (with $\alpha_t \lesssim 0.3$ typically) so that the pressure profile scales as $P_{\rm th} = nkT \propto r^{\alpha_t - 1}$. As a result, we obtain a scaling of the cooling and CR heating rates with radius of $\mathcal{C}_{\rm rad} \propto r^{-2}$ and $\mathcal{H}_{\rm CR} \propto d(r^{\alpha_t-1})/dr \propto r^{\alpha_t-2}$. Those are identical for a constant temperature ($\alpha_t = 0$). For a smoothly rising temperature profile ($\alpha_t \lesssim 0.3$) the heating rate profile is tilted and slightly favoured over the cooling rates at larger radii, provided they match up at some inner radius (see Fig. 2). A corollary of this consideration is that the onset of cooling is smoothly modulated from the outside in, as we will see in the following.

3.3. *Local Stability Analysis*

CR heating appears to be able to keep the gas in *global* thermal equilibrium in M87. However, this does not necessarily imply *local* thermal stability. We consider small isobaric perturbations to this equilibrium configuration, which maintain pressure equilibrium at each radius. The assumption of isobaric perturbations is well justified for small timescales in comparison to the dynamical timescale, $\tau_{\rm dyn} \approx (2\pi G\rho_m)^{-1/2} \approx 150\,{\rm Myr} \times n_{-2}^{-1/2}$, where $n_{-2} = 10^{-2}\,{\rm cm}^{-3}$, $\rho_m = \rho_b/f_b$ is the total matter density, ρ_b and $f_b \approx 0.166$ are the baryonic matter density and baryon-to-dark matter mass fraction, respectively. In Appendix A we derive a general instability criterion for a fluid that is cooling by thermal bremsstrahlung and line emission and heated by a generic mechanism with a power-law dependence on ρ and T while allowing for thermal and CR pressure support. We will start the discussion with a transparent order of magnitude calculation that provides insight into the physics and complements the formal treatment in Appendix A.

The generalized Field criterion (Field 1965; Balbus 1986) for thermal instability in the presence of isobaric perturbations is given by

$$\left.\frac{\partial(\mathcal{L}/T)}{\partial T}\right|_P < 0, \qquad (9)$$

where $\mathcal{L}$ is defined as the net loss function per unit mass such that $\rho\mathcal{L} = \mathcal{C} - \mathcal{H}$, where $\mathcal{C}$ and $\mathcal{H}$ are the cooling and heating rates per unit volume. On short timescales that we consider for our stability analysis, the CR population can be considered adiabatically since it does not suffer non-adiabatic losses such as hadronic interactions (e.g., Enßlin et al. 2007). In particular, CR streaming is an adiabatic process for the CR population (Enßlin et al. 2011), implying locally $P_{\rm CR} \propto \rho^{\gamma}$, where γ is the adiabatic exponent of the CR population. We emphasize that this *local* adiabatic behavior of $P_{\rm CR}$ does not hold for the *equilibrium* distribution of CRs that is subject to non-adiabatic gain and loss processes, which modify the "CR entropy" (i.e., its probability density of the microstates).[5] We obtain the scaling of the CR heating rate with temperature,

$$\mathcal{H}_{\rm CR} = -\upsilon_A \nabla P_{\rm CR} \propto \rho^{\gamma+1/3} \propto T^{-\gamma-1/3}. \qquad (10)$$

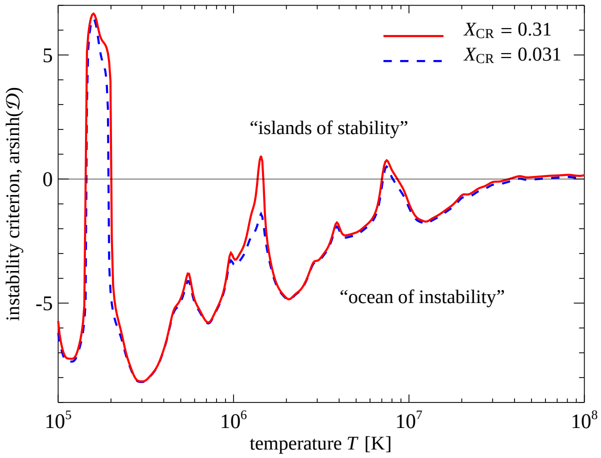

Figure 3. Local stability analysis of a fluid for which CR heating globally balances radiative cooling by bremsstrahlung and line emission (assuming solar metallicity). We show the instability criterion, $\mathcal{D} \propto \partial(\mathcal{L}/T)/\partial T|_P$, as a function of temperature for parameters appropriate for M87 (red) and for a ten times lower CR pressure (blue dashed). Precisely, we show arsinh($\mathcal{D}$), which has a linear (logarithmic) scaling for small (large) values of the argument. Once the gas temperature drops below 3×10^7 K, it becomes thermally unstable. Assuming that the gas cools while maintaining approximate thermal equilibrium, its collapse is halted at around 10^7 K by the first "island of stability", which is consistent with the temperature floor seen in x-ray observations. However, the high-density tail of density fluctuations should able to cross this island and become again subject to thermal instability, likely sourcing some of the observable multi-phase gas.

Here we identified the characteristic size of our unstable clump with an exponential pressure scale height h so that the local gradient length scales as $\delta l \sim h \propto \rho^{-1/3}$ and we assumed $\upsilon_A = {\rm const}$. We suppress the dependence on pressure, which is constant for isobaric perturbations. The radiative cooling rate scales with temperature as

$$\mathcal{C}_{\rm rad} = \rho^2 \left[\Lambda_0 Z^2 T^{1/2} + \Lambda_l(T,Z)\right] \propto T^{-3/2} + \eta T^{-2+\chi}, \qquad (11)$$

where the first and second term in the brackets denote the bremsstrahlung and line-emission cooling. Here we introduce the logarithmic temperature slope of the line cooling function χ and the ratio of line-to-bremsstrahlung cooling rate η. For an ultra-relativistic CR population with $\gamma = 4/3$, we find a stable fixed point in the bremsstrahlung regime since the slope of the heating rate ($= -5/3$) is steeper than that of the cooling rate ($= -3/2$). Increasing (decreasing) the temperature of a perturbed parcel of gas implies a stronger cooling (heating) that brings the parcel back to the background temperature. However in the line-cooling regime (at $(1-3) \times 10^7$ K), which is characterized by $\eta \gtrsim 1$ and $\chi \lesssim 0$, the slope of the cooling rate ($\lesssim -2$) is steeper than that of the CR heating rate ($= -5/3$), implying instability.

This simple order of magnitude calculation is substantiated in Fig. 3, which shows the instability criterion derived in Equation (A11) and restricted to CR Alfvén wave heating as the sole source of heat in the central region of the Virgo cluster. A gas in thermal equilibrium ($\rho\mathcal{L} = 0$) is thermally unstable if

$$\mathcal{D} \equiv \frac{1}{2} + \eta\chi - \frac{(5/3-\gamma)(1+\eta)}{1 + X_{\rm CR}\gamma} < 0. \qquad (12)$$

We compute the logarithmic temperature slope of the line cooling function $\chi(T)$ and the ratio of line-to-bremsstrahlung cooling rate $\eta(T)$ for a gas at solar metallicity and assume collisional ionization equilibrium (Sutherland & Dopita 1993). In Fig. 3, we show $\mathcal{D}$ as a function of temperature and adopt values appropriate for M87 ($\gamma = 1.37$ and $X_{\rm CR} = 0.31$, see Appendix A.2). For most of the temperature range, we find that $\mathcal{D} < 0$ and the gas is subject to thermal instability. However, there are a few "islands of stability" where $\mathcal{D} > 0$.

---

[5] This is similar to thermal cluster gas that increases its pressure $P_{\rm th} \propto \rho^{5/3}$ upon adiabatic changes. However, non-adiabatic processes such as shocks triggered by gravitational infall, non-gravitational heating, and radiative cooling modify the gas entropy. As a result, the gas obeys an effective adiabatic exponent $\gamma_{\rm eff} \equiv \partial \ln P_{\rm th}/\partial \ln \rho \approx 1.1 - 1.3$ within a cluster that only slowly increases beyond the radii of accretion shocks toward the adiabatic value (e.g., Battaglia et al. 2010; Capelo et al. 2012).

The location of such an "island of stability" corresponds to a sufficiently positive slope of the cooling function $\Lambda_{\rm cool}$ as a function of T (i.e., it is located at the low-temperature side of every line-cooling complex). Increasing the metallicity Z increases the cooling rate and sharpens the line complexes. This implies more stable "islands of stability", i.e., they protrude more above the "ocean of instability", but they also extend over a slightly smaller temperature range. However, increasing Z does not significantly change their localization in temperature (as long as the CR heating can compensate the increasing cooling rate that accompanies the elevated Z).

Apart from parameters associated with radiative cooling (e.g., metallicity), $\mathcal{D}$ also depends on cluster-immanent parameters associated with the CR distribution, i.e., the CR adiabatic exponent γ and the CR-to-thermal pressure ratio $X_{\rm CR}$. Of those, only $X_{\rm CR}$ can in principle vary substantially among clusters. To address the robustness of the shape of the instability criterion $\mathcal{D}$ with respect to variations in $X_{\rm CR}$, in Fig. 3 we additionally show $\mathcal{D}$ for a ten times lower CR pressure (which would however not suffice to maintain global thermal equilibrium in M87). Most importantly, the shape of $\mathcal{D}$ versus temperature barely changes, except that the second "island of stability" vanishes for low values of $X_{\rm CR}$.

3.4. *A Critical Length Scale for the Instability*

Before we can discuss the fate of the cooling gas, we will be considering the typical length scale of a region that becomes subject to thermal instability. We expect cooling gas parcels only to appear in systems whose dimension is greater than a critical length scale $\lambda_{\rm crit}$, below which CR Alfvén wave heating smoothes out temperature inhomogeneities. We will estimate $\lambda_{\rm crit}$ by considering thermal balance for a cool parcel of radius r embedded in a medium with an equilibrium CR pressure $P_{\rm CR} = X_{\rm CR} P_{\rm th}$. CR streaming transfers an amount of energy to a given parcel at a rate $\sim r^3 f_s \upsilon_A (P_{\rm CR}/r)$, where f_s is a suppression factor that depends on the magnetic topology connecting the parcel with its surroundings. Line emission and bremsstrahlung cooling can radiate energy from the cloud at a rate $\sim r^3 n_e n_t \Lambda_{\rm cool}(Z,T)$. Cooling and CR heating are thus approximately balancing each other for systems with a radius

$$\lambda_{\rm crit} = \frac{f_s \upsilon_A P_{\rm CR}}{n_e n_t \Lambda_{\rm cool}} = \frac{f_s X_{\rm CR}}{\mu_t} \frac{\upsilon_A kT}{n_e \Lambda_{\rm cool}}, \tag{13}$$

where $\mu_t = n_t/n = (3X_{\rm H}+1)/(5X_{\rm H}+3) \simeq 0.48$ assuming primordial element composition.

In Fig. 4 we show $\lambda_{\rm crit}$ as a function of radius for the parameters of M87 used throughout, i.e., $\upsilon_A = 130$ km s^{-1}, $X_{\rm CR} = 0.31$, $\Lambda_{\rm cool}(T_0, Z_0)$ of Section 3.2, and the observed electron temperature and density profiles of Equations (2) and (3). The CR heating rate without azimuthal fluctuations ($f_{\rm sup} = 1$) yields a critical wavelength $\lambda_{\rm crit} > r$ at all radii, which implies that the unstable wavelengths cannot be supported by the cluster core.

Since CRs stream anisotropically along magnetic fields, this may suppress the heating flux into a given volume element depending on the magnetic connectivity to the surroundings. In the case of an isotropically tangled small-scale magnetic field, CR heating along a given direction is suppressed by a factor $f_{\rm sup} \approx 0.3$. As a result, the minimum size of an unstable region at 10 kpc is $\lambda_{\rm crit} = 5-8$ kpc, depending on metallicity. However, such a large region is unlikely to be exclusively heated from one direction, which makes it challenging for cooling multiphase gas to form unless a given regions is sufficiently magnetically insulated with a suppression factor $f_{\rm sup} \ll 1$. Since we have demonstrated in Fig. 2 that CR heating globally balances cooling, a magnetic suppression of heating into one region implies an overheating in another. Because the gas is thermally unstable for temperatures in the range of $(1-3)\times 10^7$ K, the additional energy would be radiated away on the radiative cooling time.

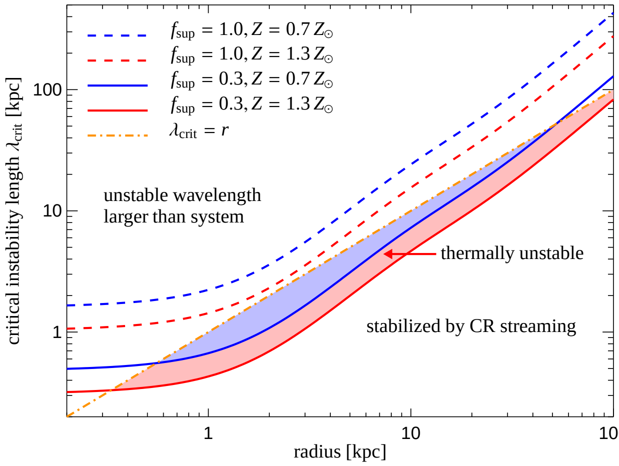

Figure 4. Radial dependence of the critical instability length scale $\lambda_{\rm crit}$ that is obtained by balancing the CR heating rate $\mathcal{H}_{\rm CR}$ with the radiative cooling rate $\mathcal{C}_{\rm rad}$. On scales $\lambda < \lambda_{\rm crit}$, CR heating dominates over cooling and wipes out any temperature inhomogeneities. Gas parcels on scales $\lambda > \lambda_{\rm crit}$ can become thermally unstable unless $\lambda > r$, for which the unstable wavelengths cannot be supported by the system. To compute the radiative cooling, we vary the abundance of the gas between $Z = 0.7 Z_\odot$ (blue) and $Z = 1.3 Z_\odot$ (red). We show one case without azimuthal fluctuations in the CR heating rate (dashed) and one with magnetic suppression by a factor $f_{\rm sup} = 0.3$ (solid).

3.5. *The Emerging Physical Model of a "Cooling Flow"*

The previous considerations enable us to construct a comprehensive "cooling flow" model for M87, which may serve as a blueprint for other CC clusters. We distinguish three different cases, each of which may be realized by a different magnetic suppression factor. However, quantifying their relative abundance requires appropriate numerical simulations.

Case A. In the absence of strong magnetic suppression of the CR heat flux, a gas parcel is thermally stabilized by CR heating because the system cannot support the unstable wavelengths, which are larger than the cluster radius.

Case B. For strong magnetic suppression of the CR heat flux, gas at temperatures $T = (1-3)\times 10^7$ K is thermally unstable, starts to cool radiatively, becomes denser than the ambient gas and begins to sink toward the center. Since CRs are largely confined to stay on individual field lines, which are flux frozen into the contracting gas, the CR population is adiabatically compressed. This implies an increasing CR heating rate $\mathcal{H}_{\rm CR} \propto \rho^{\gamma+1/3}$ (Equation 10), which however increases at a slower rate than the cooling rate for $T = (1-3)\times 10^7$ K (see Section 3.3). The CRs transfer energy to the gas on a timescale comparable to the Alfvén crossing time over the CR pressure gradient length, $\tau_A = \delta l/\upsilon_A \sim 75$ Myr for $\delta l = 10$ kpc.

If the gas parcel remains magnetically insulated, it cannot be supplied with a fresh influx of CRs, which causes the CR heating to lag the radiative cooling, implying eventually the formation of multi-phase gas and potentially stars, provided favourable conditions for their formation are met. Such a magnetic suppression could be realized through processes that dynamically form coherently aligned magnetic sheaths, which are wrapped around the gas parcel as a result of either the action of magnetic draping (Lyutikov 2006; Ruszkowski et al. 2007; Dursi & Pfrommer 2008), the heat-flux driven buoyancy instability (Quataert 2008; Parrish & Quataert 2008), or through radial collapse, which amplifies the azimuthal components of the magnetic field, in combination with coherent motions of the cooling gas parcel so that the azimuthal magnetic field becomes causally unconnected to its surroundings.

The comparably large critical wavelength of the instability, $\lambda_{\rm crit}$, at large radii (even for substantial magnetic suppression) may make it difficult for thermal instability to condense out large gas clouds (which requires a stable magnetic insulation on the correspondingly long timescale τ_A). Instead, it is more likely that cooling (multi-phase) clouds form in the central regions at radii $\lesssim 3$ kpc because of the small $\lambda_{\rm crit}$. For this case, the presence of small pockets of multi-phase gas at larger radii will then necessarily imply that they would have to be uplifted by eddies driven by the rising radio cocoons.

Case C. For moderate magnetic suppression of a given gas parcel at $T = (1-3)\times10^7$ K, CR heating will be able to approximately match radiative cooling. That means we can consider the gas parcel to be in global thermal equilibrium but subject to local thermal instability. If this global thermal equilibrium can be maintained during the cooling of a necessarily large region of wavelength $\lambda \sim r$, and if the perturbations are in pressure equilibrium with the surroundings, then the results of our stability analysis applies. In particular, the gas collapse is halted at around 1 keV by the first "island of stability" (situated at $T_{\rm floor} = (0.7-1)\times10^7$ K). Hence for *case C*, we predict a temperature "floor" at the cluster center with typical values distributed within $T_{\rm floor}$. The insensitivity of the shape of the first "island of stability" on the various parameters entering the instability criterion suggests that we found a universal mechanism that sets a lower temperature floor in CC clusters (as long as the CR pressure is sufficient to provide global thermal stability).

This prediction of a generic lower temperature floor at $T_{\rm floor}$ is in agreement with high-resolution x-ray observations of Virgo (Matsushita et al. 2002; Million et al. 2010), suggesting a viable solution for the puzzling absence of a large amount of lower-temperature gas in Virgo that is expected for an unimpeded cooling flow. However, gas in the high-density tail of density fluctuations can cool below $T \simeq 0.7\times10^7$ K, and hence leave this "island of stability". These dense fluctuations again become subject to thermal instability, sourcing some of the observable multi-phase gas (Werner et al. 2010, 2012). The collapse could again be halted at the second and third "island of stability" just above 10^5 K and 10^6 K. However, since cooling clouds at these temperatures are associated with higher densities and smaller length scales, the amount of CR heating now depends critically on the magnetic connectivity of the cloud with the surroundings since that determines whether there will be a sufficient influx of CRs responsible for sustaining the heating rate.

We emphasize that the success of our model came about without any tunable parameters and only used input from nonthermal radio and gamma-ray observations. The model implies that gas in the core region of Virgo is in global equilibrium but susceptible to local thermal instability. Hence this provides a physical foundation of the phenomenological prescription used in numerical simulations that study the interplay of thermal instability and feedback regulation (McCourt et al. 2012; Sharma et al. 2012). There are also notable differences since these prescriptions did not have the modulating effect of our "islands of stability". We may speculate that our model may then inherit some of their successes including quantitative consistency with data on multi-phase gas and star formation rates but holds the promise to cure the problem of the absence of a (physical) temperature floor in these numerical experiments.

4. OBSERVATIONAL PREDICTIONS

This model makes several predictions for gamma-ray, radio, and Sunyaev-Zel'dovich observations, which we will discuss in turn. Some of the proposed observations may first be possible in M87, owing to its immediate vicinity. To address the universality of the this heating mechanism, these observations are certainly worthwhile to be pursued in other nearby CC cluster that show strong signs of AGN feedback.

4.1. *Gamma Rays*

If the gamma-ray emission of the low-state of M87 results from hadronic CRp-p interactions then the emission should be extended with a characteristic angular profile worked out by Pfrommer & Enßlin (2003) for their isobaric CR model. The gamma-ray emission should not show any sign of time variability and should be characterized by the distinct spectral signature of decaying pions around 70 MeV (in the differential spectrum). The triad of these observations will prove the existence of CRps mixed into the ICM and measure their pressure contribution. Spatially resolving the gamma-ray emission helps in estimating the large-scale CR pressure gradient and its contribution to the CR-heating rate. However, this does not shed light on the contribution from small-scale pressure fluctuations. The comparably coarse angular resolution of *Fermi* (68% containment angle of $12'$ above 10 GeV) precludes such a measurement in M87. In contrast, the superior resolution of current and future Cerenkov telescopes (radius of a circle enclosing 80% of the light is $1.4'$ with H.E.S.S. II above TeV energies and expected to be five times better with CTA) is a promising route toward measuring the pressure gradient of the high-energy CRps, which however carry only a small amount of the total pressure that is dominated by the GeV-energy regime.

We note that a critical prediction of this model is the similarity of the spectral indexes of the gamma-ray emission above GeV energies (which corresponds to that of the CR population) and the injection index of the CRe population, as probed by low-frequency radio observations of the core regions of Virgo A. Similar observations of nearby AGNs in CC clusters are necessary to show the universality of the presented mechanism.

4.2. *Radio Emission*

Faraday rotation measurements of background sources or polarized regions of Virgo A (central region, halo, or rising cocoons) will provide not only a reliable estimate of the spatial distribution of field strengths, but also about the magnetic morphology. This is important for predicting the heating rates (that scale with the Alfvén velocity) and the microphysics of CR Alfvén wave heating, which depends on in situ alignments of magnetic fields with the CR pressure gradients. In particular, CR release time scales from the radio cocoons may depend on the pre-existing morphology of the magnetic fields that dynamically drape around a super-alfvénically rising cocoon (Lyutikov 2006; Ruszkowski et al. 2007). This magnetic draping effect stabilizes the interfaces against the shear that creates it in first place (Dursi 2007). However, magnetic draping can only occur if the ratio of the integral length scale of the magnetic power spectrum λ_B and the curvature radius R of the radio cocoon at the stagnation line obeys the relation (see Supplementary Information of Pfrommer & Dursi 2010)

$$\frac{\lambda_B}{R} \gtrsim \mathcal{M}_A^{-1} = \left(\mathcal{M}\sqrt{\frac{\gamma\beta}{2}}\right)^{-1} \simeq 0.25\,\mathcal{M}^{-1}\left(\frac{\beta}{20}\right)^{-1/2}, \tag{14}$$

where $\mathcal{M}$ and $\mathcal{M}_A$ are the sonic and Alfvénic Mach numbers of the rising cocoons, $\gamma = 5/3$, and β is the plasma beta factor. The violation of this relation could cause Kelvin-Helmholtz and Rayleigh-Taylor instabilities to shred the cocoons and to release CRs into the ICM. Higher-order Faraday rotation measure statistics are sensitive to the statistics of the projected magnetic field distribution. Complementary to this are magnetic draping studies at spiral galaxies within this central region (Pfrommer & Dursi 2010) that provide a means of measuring the projected *in situ* geometry of the magnetic field at the galaxies' position. Additionally, those could be of paramount importance to provide indications for a spatially preferred direction of magnetic fields which could hint at the presence of a magnetic buoyancy instability.

The hadronic CRp-p reaction also implies the injection of secondary CRes that contribute to the radio synchrotron emission with a spectral index that reflects the CRp proton distribution (i.e., $\alpha_\nu = (\alpha-1)/2 = 0.63$ in M87). Using the formalism of Pfrommer et al. (2008), we calculate the hadronically-induced radio halo emission within a spherical region of radius 34 kpc (adopting the same parameters as in the rest of the paper, namely $X_{\rm CR} = 0.31$, $\alpha = 2.26$, $q = 0.58$ and the model for the magnetic field of Section 3.1). At 1.4 GHz (10.55 GHz), this emission component is expected to have a total flux density of 21.1 Jy (2.15 Jy), which falls short of the observed halo emission by a factor of 6.6 (10) (see Figures 10 and 11 of de Gasperin et al. 2012).

However, the spatial profile of the expected hadronically-induced emission is very different from the observed radio halo emission, which is centrally more concentrated. If we exclude a cylinder centered on the central radio cocoon of radius 2.5 kpc (corresponding to $0.51'$), we obtain a flux density at 1.4 GHz (10.55 GHz) for the external hadronic halo of 19.8 Jy (2.0 Jy), which compares favorably to the observed emission of 69.1 Jy (3.4 Jy) that subtends the same solid angle (Figure 11 of de Gasperin et al. 2012). In particular, the hadronically-induced emission is expected to make up $\sim 60\%$ of the observed (external) halo emission at 10.55 GHz. Clearly, the possibility of such an emission component should be accounted for when drawing conclusions about the CRe pitch angle distribution in spectral ageing models of synchrotron and inverse Compton emitting CRes (de Gasperin et al. 2012), especially if the high-frequency data is sparse so that individual data points impart high statistical weights in the fits.

If CR electrons and protons have a very different distribution within the radio halo (which could be achieved through enhanced radiative losses of CRes in regions of strong magnetic fields), there may be regions in which hadronically-induced emission prevails over the primary emission. Those regions should then show a radio spectral flattening in comparison to the adjacent primary emission-dominated regions. Because of the flatter slope of the hadronically-induced emission, such a measurement may be even more promising at high radio frequencies $\nu \gtrsim 10$ GHz.

4.3. *Sunyaev-Zel'dovich observations*

High-resolution Sunyaev-Zel'dovich studies can reveal the composition of the plasma within radio cocoons (Pfrommer et al. 2005). This could unambiguously demonstrate the presence of CRs in bubbles which would imprint as high-contrast cavities in high-resolution Sunyaev-Zel'dovich maps at the radio cocoons' positions. Their signature is different from the hypothetical alternative of a hot, but sub-relativistic particle population. However, the large dynamic range required for such a detection in Virgo A will make such a measurement very challenging.

5. DISCUSSION AND CONCLUSIONS

What is *the* dominant physical mechanism that quenches cooling flows in CC clusters? Over the last decade, many different processes have been proposed. We will discuss the pros and cons of the major contenders that are representative of generic classes of heating models. For the first time, we have proposed a comprehensive CC heating model that not only convincingly matches radio, x-ray, and gamma-ray data for M87 but is also virtually free of tunable parameters. In particular, our global and local stability analyses of the CR heating model reveal generic aspects that may apply universally to CC clusters, provided the CR release timescales from the radio cocoons are similar to that in M87.

5.1. *Overview of Solutions to the "Cooling Flow Problem"*

Thermal conduction of heat from the hot outer cluster regions to the cooling cores has been proposed to solve the problem (Narayan & Medvedev 2001; Zakamska & Narayan 2003). However, there are a number of drawbacks of this proposal. (1) The strong temperature dependence of thermal conductivity ($\kappa \propto T^{5/2}$) makes this a very inefficient process for groups and small clusters. (2) Thermal conduction ceases to be important if gas cools to low temperatures and, as such, requires in some clusters a conductivity above the classical Spitzer value as well as a high degree of fine tuning (Voigt & Fabian 2004; Conroy & Ostriker 2008). (3) The heat-flux-driven buoyancy instability (Quataert 2008) causes the magnetic field lines to align with the gravitational equipotential surfaces of the cluster in the non-linear stage of the instability (Parrish & Quataert 2008). At first sight, this should suppress the inward transport of heat by more than an order of magnitude and should reinforce the cooling flow problem. The instability, however, is easily quenched by the presence of external turbulence at the level of $\sim 1\%$ of the thermal pressure (Parrish et al. 2010; Ruszkowski & Oh 2010), leaving the question of how much thermal conduction is suppressed by the presence of magnetic fields in realistic cosmological situations. Overall, thermal conduction could certainly aid in mitigating the fast onset of cooling at intermediate cluster radii (Voit 2011) but is unlikely to play a major role in the cluster centers.

Over the last years, AGN feedback has become the lead actor because of its promising overall energetics and the observational confirmation that the nuclear activity appears to be tightly coupled to a self-regulated feedback loop (Bîrzan et al.

2004). Guided by high-resolution *Chandra* x-ray observations, which emphasize sharp density features in high-pass filtered maps as a result of the gas being pushed around by AGN jets and cocoons, many papers have focused on the dissipation of *PdV* work done by the inflating cocoon on the surroundings. The detailed heating mechanisms include sound waves, weak shocks, and turbulence (see McNamara & Nulsen 2012, and references therein). Since sound waves and weak shocks are excited in the center by the AGN, their outward-directed momentum flux in combination with the small dissipation efficiency implies that only a small fraction of this energy will be used for heating the central parts. Those parts, however, have the lowest cooling time. Additionally, the implied heating rate is very intermittent in space and time with an unknown duty cycle. Nevertheless, these processes will certainly happen and (if the outburst energy is large enough) may locally even dominate during some times (Nulsen et al. 2005). As we argue in this paper, these processes are however unlikely to be the most important heating source because they do not provide a generic solution to the lower temperature floor observed in CCs and they are not favored on energetic grounds due to their small heating efficiency.

Assuming a relativistic filling of the cocoons, three quarters of the total cocoon enthalpy is stored in internal energy. We provide arguments in favor of a CRp population that dominates the internal cocoon pressure. Once released, those CRp stream at about the Alfvén velocity with respect to the plasma rest frame and excite Alfvén waves through the "streaming instability" (Kulsrud & Pearce 1969). Damping of these waves transfers CR energy and momentum to the thermal gas at a rate that scales with the product of the Alfvén velocity and the CR pressure gradient (Guo & Oh 2008). While very plausible, there was the open question of whether the CRp population has been mixed into the ICM and whether it is abundant enough to provide sufficiently strong heating to offset the cooling catastrophe. In this paper, we answer both questions affirmatively for the case of M87 on the basis of a detailed analysis of non-thermal observations. Moreover, in addressing the issue of local thermal stability in this model, we put forward an attractive solution to the problem of an apparent temperature floor in CC clusters.

5.2. *Cosmic Ray Heating as the Solution?*

The puzzling absence of fossil CRes implied by the LOFAR observations of M87 can be naturally explained by the observed shredding of radio cocoons during their rise in the gravitational potential, e.g., through the action of Kelvin-Helmholtz and Rayleigh-Taylor instabilities. This releases and mixes CR electrons and protons into the ambient dense ICM. We argue that mixing is essential in this picture so that the CRes have direct contact with the dense ambient plasma, which causes CRes to efficiently cool through Coulomb interactions. This implies a maximum CRe cooling time scale of $\simeq 40$ Myr, which is similar to the age of the Virgo A radio halo. A direct consequence of this interpretation is that CRps are similarly mixed with the dense gas and must collide inelastically with gas protons. This produces pions that decay into a steady gamma-ray signature, which resembles that of the flux in the "low state" of M87 observed by *Fermi* and H.E.S.S. In particular, the CRp population (witnessed through the gamma-ray emission) shares the same spectral index as the injected CRe population in the core region of Virgo A, which we consider as strong support for a common origin of the radio and gamma-ray emission.[6] Hence, the hadronically induced gamma-ray emission enables us to estimate the CR pressure, which has a CR-to-thermal pressure contribution of $X_{\rm CR} = 0.31$ (allowing for a conservative Coulomb cooling timescale of order the radio halo age that modifies the low-energy part of the CRp distribution).

We show that streaming CRs heat the surrounding thermal plasma at a rate that balances that of radiative cooling *on average* at each radius. Hence, the thermal pressure profile is a consequence of the interplay of CR heating and radiative cooling and should match that of the streaming CRs (hence justifying in retrospect our assumption of a constant CR-to-thermal pressure in our analysis). We argue that this similar radial scaling of the heating and cooling rate profiles is not a coincidence in M87 but rather generically expected in models of CR Alfvén wave heating.

However, the *global* thermal equilibrium is *locally* unstable if the gas temperature drops below $kT \simeq 3$ keV (for solar metallicity). The fate of a gas parcel depends on its magnetic connectivity to the surroundings, which may obey a yet unknown distribution function. Nevertheless, we can distinguish three different cases.

(1) For magnetically well-connected patches without appreciable fluctuations in the CR heating rate, temperature inhomogeneities are smoothed out on scales smaller than the cluster-centric radius. As a result, the system is stabilized because it cannot support the unstable wavelengths.

(2) Contrarily, for strong magnetic suppression of the CR heat flux, the thermally unstable gas starts to cool radiatively, becomes denser than the ambient gas, and sinks toward the center. After an initial phase when the magnetically trapped CRs within the parcel deposit their energy to the gas, CR heating lags cooling. This eventually causes the formation of multi-phase gas and potentially stars. At large radii, the critical wavelength $\lambda_{\rm crit}$ above which thermal instability can operate is comparably large, thereby making it more likely for multi-phase gas to form further inward where $\lambda_{\rm crit}$ is smaller. Thus, small clumps of multi-phase gas at larger radii would have to be uplifted by eddies driven by the rising radio cocoons.

(3) For the perhaps most probable case of moderate magnetic suppression, CR heating will be able to approximately match radiative cooling. If this global thermal equilibrium can be maintained during the Lagrangian evolution of the cooling gas parcel that is in pressure equilibrium with its surroundings, then the gas collapse is halted at around 1 keV by an "island of stability". There, the CR heating rate has a steeper dependence on temperature than the radiative cooling rate. Increasing (decreasing) the temperature of a perturbed parcel of gas implies a stronger cooling (heating) that brings the parcel back to the background temperature. This is consistent with the observed temperature floor of $0.7-1$ keV seen in the x-ray observations of the center of Virgo. Since this result is insensitive to significant variations of the CR pressure support, this may suggest a viable solution to the "cooling flow problem" (as long as the CR heating rate is sufficient to provide global thermal stability).

However, the high-density tail of density fluctuations that is associated with temperatures $kT \lesssim 0.7$ keV becomes again subject to thermal instability, thereby providing a plausible mechanism for the formation of some of the observed cooling multiphase medium in and around M87. We note that the success of the CR heating model came about without any tunable parameters and *only* used input from radio and gamma-ray observations. We present several testable predictions of this model that include gamma-ray, radio, and Sunyaev-Zel'dovich observations.

---

[6] As de Gasperin et al. (2012), we interpret the steeper CRe spectra in the halo of Virgo A as a result of a superposition of CRe spectra with different radiative cooling breaks that they attained during their transport from the core region, which is an effect that should leave the CRp spectra invariant.

We emphasize the importance of non-thermal observations to establish this physical picture of AGN feedback and to pinpoint the details of this heating mechanism in M87. While tempting, we caution against directly extrapolating our result to other CC clusters. To faithfully do so, we would need similar non-thermal observations to establish that CRs are injected and mixed into the ambient ICM and to estimate the CR pressure contribution that determines the CR heating rate. In particular, CR release time scales from the radio cocoons are crucial and may depend on the pre-existing morphology of the magnetic fields that dynamically drape around the rising cocoons (Ruszkowski et al. 2007). Those draped fields provide stability in the direction of the magnetic field against the shear that creates it if the magnetic coherence scale is large enough for draping to be established in the first place. Future Faraday rotation measure studies and galaxy draping observations (Pfrommer & Dursi 2010) may help to clarify this point.

We hope that this work motivates fruitful observational and theoretical efforts toward consolidating the presented picture and to establish non-thermal observations of the underlying high-energy processes as a driver for the understanding of the evolution of cluster cores and perhaps the modulation of star formation in elliptical galaxies.

I thank Ewald Puchwein and Volker Springel for critical reading of the manuscript and helpful suggestions. I thank Heino Falcke and Frank Rieger for discussions and gratefully acknowledge financial support of the Klaus Tschira Foundation.

APPENDIX

A. THERMAL STABILITY IN THE PRESENCE OF A RELATIVISTIC FLUID

A.1. Balancing Bremsstrahlung and Line Cooling by Generic Heating Mechanisms

Consider a fluid subject to external heating and cooling. The generalized Field criterion (Field 1965; Balbus 1986) for thermal instability in the presence of isobaric perturbations is given by

$$\left.\frac{\partial(\mathcal{L}/T)}{\partial T}\right|_P < 0. \tag{A1}$$

Here $\mathcal{L}$ is the net loss function in units of ergs s^{-1} g^{-1} defined such that $\rho\mathcal{L} = \mathcal{C} - \mathcal{H}$, where $\mathcal{C}$ and $\mathcal{H}$ are the cooling and heating rates per unit volume. $\mathcal{L}$ is generally a function of gas mass density ρ, temperature T, and possibly space and time. We study the instability in the presence of a relativistic fluid and generalize the derivation by Conroy & Ostriker (2008) to also include cooling by line emission in addition to thermal bremsstrahlung, which will turn out to be important for putting the complete picture in place (in particular for cooling flows in clusters).

A gas in thermal equilibrium ($\rho\mathcal{L} = 0$) obeys the following identity,

$$\left.\frac{\partial(\mathcal{L}/T)}{\partial T}\right|_P = \frac{1}{\rho T}\left[\left.\frac{\partial(\rho\mathcal{L})}{\partial T}\right|_\rho + \left.\frac{\partial\rho}{\partial T}\right|_P \left.\frac{\partial(\rho\mathcal{L})}{\partial\rho}\right|_T\right]. \tag{A2}$$

The first and third derivatives on the right-hand side are governed by the heating and cooling processes under consideration, while the second depends on the various sources of pressure support. We consider pressure support provided by thermal gas and a relativistic fluid (dominated by CRps):

$$P = P_{\mathrm{th}} + P_{\mathrm{CR}} = K_1\rho T + P_{\mathrm{CR}}(\rho), \tag{A3}$$

where K_1 is a constant and P_{CR} is only a function of density. We use the following identity

$$\left.\frac{\partial\rho}{\partial T}\right|_P = -\left.\frac{\partial P}{\partial T}\right|_\rho \left(\left.\frac{\partial P}{\partial\rho}\right|_T\right)^{-1} \tag{A4}$$

to obtain

$$\left.\frac{\partial\rho}{\partial T}\right|_P = -\frac{K_1\rho}{K_1 T + \left.\left(\partial P_{\mathrm{CR}}/\partial\rho\right)\right|_T} = -\frac{\rho}{T}\frac{P_{\mathrm{th}}}{P_{\mathrm{th}} + \rho\left.\left(\partial P_{\mathrm{CR}}/\partial\rho\right)\right|_T} = -\frac{\rho}{T}\frac{1}{1 + X_{\mathrm{CR}}\left.\left(\partial\ln P_{\mathrm{CR}}/\partial\ln\rho\right)\right|_T}, \tag{A5}$$

where we defined $X_{\mathrm{CR}} \equiv P_{\mathrm{CR}}/P_{\mathrm{th}}$.

We now assume that the heating has a power-law dependence on ρ and T and account for cooling by thermal bremsstrahlung and line emission to get

$$\rho\mathcal{L} = \mathcal{C}_{\mathrm{rad}} - \mathcal{H} = \rho^2\left[\Lambda_b(T,Z) + \Lambda_l(T,Z)\right] - \Gamma_0\rho^\beta T^{-1/2+\delta}, \tag{A6}$$

where $\Lambda_b(T,Z) = \Lambda_0 Z^2 T^{1/2}$ and $\Lambda_l(T,Z)$ are the cooling functions due to bremsstrahlung and line emission, respectively. Both depend on metallicity and temperature. (For brevity, we omit the arguments in the following.) Λ_0 and Γ_0 are constants, and we define the identical power-law indices δ and β for the heating as in Conroy & Ostriker (2008) to ease comparison with their results. Using the relation for thermal equilibrium ($\rho\mathcal{L} = 0$), we have

$$\left.\frac{\partial(\rho\mathcal{L})}{\partial T}\right|_\rho = \Lambda_b\rho^2 T^{-1}\left[1 - \delta + \frac{\Lambda_l}{\Lambda_b}\left(\left.\frac{\partial\ln\Lambda_l}{\partial\ln T}\right|_\rho + \frac{1}{2} - \delta\right)\right] \tag{A7}$$

and

$$\left.\frac{\partial(\rho\mathcal{L})}{\partial\rho}\right|_T = \Lambda_b\rho(2-\beta)\left(1+\frac{\Lambda_l}{\Lambda_b}\right). \tag{A8}$$

Combining those with Equations (A2) and (A5), we finally obtain

$$\left.\frac{\partial(\rho\mathcal{L})}{\partial T}\right|_P = \Lambda_b\rho T^{-2}\left[1-\delta+\frac{\Lambda_l}{\Lambda_b}\left(\left.\frac{\partial\ln\Lambda_l}{\partial\ln T}\right|_\rho+\frac{1}{2}-\delta\right)-\frac{2-\beta}{1+X_{\mathrm{CR}}\gamma}\left(1+\frac{\Lambda_l}{\Lambda_b}\right)\right]. \tag{A9}$$

To simplify the instability criterion, we define the logarithmic density slope of the CR pressure γ, the logarithmic temperature slope of the line cooling function χ, and the ratio of line-to-bremsstrahlung cooling, η:

$$\gamma \equiv \left.\frac{\partial\ln P_{\mathrm{CR}}}{\partial\ln\rho}\right|_T, \qquad \chi=\chi(T,Z)\equiv\left.\frac{\partial\ln\Lambda_l}{\partial\ln T}\right|_\rho, \quad \text{and} \quad \eta=\eta(T,Z)\equiv\frac{\Lambda_l}{\Lambda_b}. \tag{A10}$$

Thus, the gas is thermally unstable if the discriminant $\mathcal{D}$ is negative:

$$\mathcal{D}\equiv 1-\delta+\eta\left(\chi+\frac{1}{2}-\delta\right)-\frac{(2-\beta)(1+\eta)}{1+X_{\mathrm{CR}}\gamma}<0. \tag{A11}$$

For $\eta=0$ we recover the result of Conroy & Ostriker (2008) if we identify $X_{\mathrm{CR}}\equiv 1/\alpha'$ in their notation. Clearly, the presence of line cooling ($\eta>0$) can substantially modify the instability criterion, depending on the temperature slope χ.

A.2. Thermal Stability of a Radiatively Cooling Gas Heated by Cosmic Ray-Excited Alfvén Waves

Now, we specify this instability criterion to our case at hand of CR Alfvén wave heating. On short timescales that we consider for our stability analysis, the CR population can be considered adiabatically since it does not suffer non-adiabatic losses such as hadronic interactions. In particular, CR streaming is an adiabatic process for the CR population (Enßlin et al. 2011), implying that the CR pressure only scales with the gas density as $P_{\mathrm{CR}}\propto\rho^\gamma$ yielding

$$\mathcal{H}_{\mathrm{CR}}=\Gamma_0\rho^\beta T^{-1/2+\delta}=-\upsilon_A\nabla P_{\mathrm{CR}}\propto\rho^{\gamma+1/3}. \tag{A12}$$

Here we identified the characteristic size of our unstable clump with an exponential pressure scale height h so that the local gradient length scales as $\delta l\sim h\propto\rho^{-1/3}$ and we assume $\upsilon_A=$ const. as we do in the reminder of this work. In practice, υ_A may inherit a weak density scaling depending on the topology of the magnetic field that is compressed or expanded. We defer dynamical simulations of this interacting CR-MHD system to future work. Equation (A12) defines the power-law indices $\beta=\gamma+1/3$ and $\delta=1/2$ for the heating rate. We emphasize that this local adiabatic behavior of P_{CR} may not hold for the equilibrium distribution that is subject to gain and loss processes, which modify the “CR entropy” (i.e., its probability density of the microstates). In fact, we argued in the main part of the paper that CR Alfvén wave heating establishes an equilibrium distribution that is characterized by $X_{\mathrm{CR}}=P_{\mathrm{CR}}/P_{\mathrm{th}}\simeq$ const. *if* the dominant heating source is provided by CRs.

To estimate the CR adiabatic exponent, we remind ourselves of the definition of the CR pressure of a CR power-law population defined in Equation (1), which is given by

$$P_{\mathrm{CR}}=\frac{m_pc^2}{3}\int_0^\infty dp\,\frac{d^4N}{dp\,d^3x}\,\frac{\upsilon}{c}\,p=\frac{C\,m_pc^2}{6}\,\mathcal{B}_{\frac{1}{1+q^2}}\left(\frac{\alpha-2}{2},\frac{3-\alpha}{2}\right), \tag{A13}$$

where $\upsilon/c=p/\sqrt{1+p^2}$ is the dimensionless velocity of the CR particle and $\mathcal{B}_x(a,b)$ denotes the incomplete beta function. The local adiabatic exponent of the CR population is obtained by taking the logarithmic derivative of the CR pressure at constant CR entropy S_{CR}

$$\gamma\equiv\left.\frac{\partial\log P_{\mathrm{CR}}}{\partial\log\rho}\right|_{S_{\mathrm{CR}}}=\frac{\rho}{P_{\mathrm{CR}}}\left(\frac{\partial P_{\mathrm{CR}}}{\partial C}\frac{\partial C}{\partial\rho}+\frac{\partial P_{\mathrm{CR}}}{\partial q}\frac{\partial q}{\partial\rho}\right)=\frac{\alpha+2}{3}-\frac{2}{3}q^{2-\alpha}\frac{\upsilon(q)}{c}\left[\mathcal{B}_{\frac{1}{1+q^2}}\left(\frac{\alpha-2}{2},\frac{3-\alpha}{2}\right)\right]^{-1}\simeq 1.37 \tag{A14}$$

where we used typical values for M87 of $\alpha=2.26$ and $q=0.58$ as derived in Section 2.2.

The ratio of line-to-bremsstrahlung cooling at 1 keV for a gas with solar abundance is approximately $\eta\simeq 3.6$ (see Fig. 8 of Sutherland & Dopita 1993), assuming collisional ionization equilibrium. We can now rewrite Equation (A11) to get a constraint for the temperature slope of the cooling function χ for which the gas can become thermally unstable,

$$\chi<-\frac{1}{2\eta}+\frac{(2-\beta)(1+\eta)}{(1+X_{\mathrm{CR}}\gamma)\,\eta}\simeq 0.13, \text{ for 1 keV and } Z=Z_\odot. \tag{A15}$$

Hence, if the cooling function is sufficiently flat or even inverted (as it can be the case in the line cooling regime) we have thermal instability. In the bremsstrahlung regime, on the contrary, the gas is in thermal equilibrium, since the criterion for instability

$$\delta>\frac{X_{\mathrm{CR}}\gamma-1+\beta}{1+X_{\mathrm{CR}}\gamma}\simeq 0.8 \tag{A16}$$

cannot be fulfilled for CR Alfvén wave heating that does not depend on temperature ($\delta=1/2$).

REFERENCES

Abdo, A. A., et al. 2009, ApJ, 707, 55

Abramowski, A., et al. 2012, ApJ, 746, 151
Ackermann, M., et al. 2010, ApJ, 717, L71
Aharonian, F., et al. 2006, Science, 314, 1424
Aleksić, J., et al. 2012, A&A, 541, A99
Arlen, T., et al. 2012, ApJ, 757, 123
Balbus, S. A. 1986, ApJ, 303, L79
Battaglia, N., Bond, J. R., Pfrommer, C., Sievers, J. L., & Sijacki, D. 2010, ApJ, 725, 91
Bîrzan, L., Rafferty, D. A., McNamara, B. R., Wise, M. W., & Nulsen, P. E. J. 2004, ApJ, 607, 800
Bîrzan, L., Rafferty, D. A., Nulsen, P. E. J., McNamara, B. R., Röttgering, H. J. A., Wise, M. W., & Mittal, R. 2012, MNRAS, 427, 3468
Blanton, E. L., Sarazin, C. L., & McNamara, B. R. 2003, ApJ, 585, 227
Böhringer, H., Briel, U. G., Schwarz, R. A., Voges, W., Hartner, G., & Trümper, J. 1994, Nature, 368, 828
Brüggen, M., & Kaiser, C. R. 2002, Nature, 418, 301
Capelo, P. R., Coppi, P. S., & Natarajan, P. 2012, MNRAS, 422, 686
Cavagnolo, K. W., Donahue, M., Voit, G. M., & Sun, M. 2009, ApJS, 182, 12
Chandran, B. D. G., & Rasera, Y. 2007, ApJ, 671, 1413
Churazov, E., Brüggen, M., Kaiser, C. R., Böhringer, H., & Forman, W. 2001, ApJ, 554, 261
Churazov, E., Forman, W., Vikhlinin, A., Tremaine, S., Gerhard, O., & Jones, C. 2008, MNRAS, 388, 1062
Churazov, E., et al. 2010, MNRAS, 404, 1165
Conroy, C., & Ostriker, J. P. 2008, ApJ, 681, 151
Croton, D. J., et al. 2006, MNRAS, 365, 11
de Gasperin, F., et al. 2012, A&A, 547, A56
Dubois, Y., Devriendt, J., Teyssier, R., & Slyz, A. 2011, MNRAS, 417, 1853
Dursi, L. J. 2007, ApJ, 670, 221
Dursi, L. J., & Pfrommer, C. 2008, ApJ, 677, 993
Enßlin, T., Pfrommer, C., Miniati, F., & Subramanian, K. 2011, A&A, 527, A99
Enßlin, T. A., Pfrommer, C., Springel, V., & Jubelgas, M. 2007, A&A, 473, 41
Field, G. B. 1965, ApJ, 142, 531
Fujita, Y., & Ohira, Y. 2012, ApJ, 746, 53
Guo, F., & Oh, S. P. 2008, MNRAS, 384, 251
Kim, W.-T., & Narayan, R. 2003, ApJ, 596, L139
Kulsrud, R., & Pearce, W. P. 1969, ApJ, 156, 445
Lyutikov, M. 2006, MNRAS, 373, 73
Matsushita, K., Belsole, E., Finoguenov, A., & Böhringer, H. 2002, A&A, 386, 77
McCourt, M., Sharma, P., Quataert, E., & Parrish, I. J. 2012, MNRAS, 419, 3319
McNamara, B. R., & Nulsen, P. E. J. 2007, ARA&A, 45, 117
—. 2012, New Journal of Physics, 14, 055023
Mei, S., et al. 2007, ApJ, 655, 144
Million, E. T., Werner, N., Simionescu, A., Allen, S. W., Nulsen, P. E. J., Fabian, A. C., Böhringer, H., & Sanders, J. S. 2010, MNRAS, 407, 2046
Narayan, R., & Medvedev, M. V. 2001, ApJ, 562, L129
Nulsen, P. E. J., McNamara, B. R., Wise, M. W., & David, L. P. 2005, ApJ, 628, 629
Owen, F. N., Eilek, J. A., & Kassim, N. E. 2000, ApJ, 543, 611
Parrish, I. J., & Quataert, E. 2008, ApJ, 677, L9
Parrish, I. J., Quataert, E., & Sharma, P. 2010, ApJ, 712, L194
Peterson, J. R., & Fabian, A. C. 2006, Phys. Rep., 427, 1
Peterson, J. R., Kahn, S. M., Paerels, F. B. S., Kaastra, J. S., Tamura, T., Bleeker, J. A. M., Ferrigno, C., & Jernigan, J. G. 2003, ApJ, 590, 207
Pfrommer, C., Chang, P., & Broderick, A. E. 2012, ApJ, 752, 24
Pfrommer, C., & Dursi, L. J. 2010, Nature Physics, 6, 520
Pfrommer, C., & Enßlin, T. A. 2003, A&A, 407, L73
—. 2004, A&A, 413, 17
Pfrommer, C., Enßlin, T. A., & Sarazin, C. L. 2005, A&A, 430, 799
Pfrommer, C., Enßlin, T. A., & Springel, V. 2008, MNRAS, 385, 1211
Pinzke, A., Pfrommer, C., & Bergström, L. 2011, Phys. Rev. D, 84, 123509
Puchwein, E., & Springel, V. 2013, MNRAS, 428, 2966
Quataert, E. 2008, ApJ, 673, 758
Reimer, O., Pohl, M., Sreekumar, P., & Mattox, J. R. 2003, ApJ, 588, 155
Rieger, F. M., & Aharonian, F. 2012, Modern Physics Letters A, 27, 30030
Romanowsky, A. J., & Kochanek, C. S. 2001, ApJ, 553, 722
Ruszkowski, M., & Begelman, M. C. 2002, ApJ, 581, 223
Ruszkowski, M., Brüggen, M., & Begelman, M. C. 2004, ApJ, 611, 158
Ruszkowski, M., Enßlin, T. A., Brüggen, M., Heinz, S., & Pfrommer, C. 2007, MNRAS, 378, 662
Ruszkowski, M., & Oh, S. P. 2010, ApJ, 713, 1332
Sharma, P., Chandran, B. D. G., Quataert, E., & Parrish, I. J. 2009, ApJ, 699, 348
Sharma, P., McCourt, M., Quataert, E., & Parrish, I. J. 2012, MNRAS, 420, 3174
Sutherland, R. S., & Dopita, M. A. 1993, ApJS, 88, 253
Voigt, L. M., & Fabian, A. C. 2004, MNRAS, 347, 1130
Voit, G. M. 2011, ApJ, 740, 28
Wentzel, D. G. 1971, ApJ, 163, 503
Werner, N., et al. 2010, MNRAS, 407, 2063
—. 2012, ArXiv:1211.6722
Wiener, J., Oh, S., & Guo, F. 2013, ArXiv:1303.4746
Zakamska, N. L., & Narayan, R. 2003, ApJ, 582, 162